arXiv:1610.03259v1 [q-fin.RM] 11 Oct 2016

Epidemics of Liquidity Shortages in Interbank Markets

Giuseppe Brandi,[1] Riccardo Di Clemente,[2] and Giulio Cimini[3,4]

[1] *Libera Università Internazionale degli Studi Sociali (LUISS) "Guido Carli", 00197 Rome, Italy**
[2] *Massachusetts Institute of Technology, MA 02139 Cambridge, United States*
[3] *IMT School for Advanced Studies, 55100 Lucca, Italy*
[4] *Istituto dei Sistemi Complessi (ISC)-CNR, 00185 Rome, Italy*

(Dated: October 12, 2016)

Financial contagion from liquidity shocks has being recently ascribed as a prominent driver of systemic risk in interbank lending markets. Building on standard compartment models used in epidemics, here we develop an EDB (Exposed-Distressed-Bankrupted) model for the dynamics of liquidity shocks reverberation between banks, and validate it on electronic market for interbank deposits data. We show that the interbank network was highly susceptible to liquidity contagion at the beginning of the 2007/2008 global financial crisis, and that the subsequent micro-prudential and liquidity hoarding policies adopted by banks increased the network resilience to systemic risk—yet with the undesired side effect of drying out liquidity from the market. We finally show that the individual riskiness of a bank is better captured by its network centrality than by its participation to the market, along with the currently debated concept of "too interconnected to fail".

I. INTRODUCTION

The 2007/2008 global financial crisis has raised important concerns on the stability of the financial system, in particular regarding its complex and interconnected nature [1–4]. Indeed, because of bilateral or indirect exposures between financial institutions, credit losses and funding shortcomings can spread through the system, with potential catastrophic consequences for the whole market [5–11]. Within this context, much attention has been devoted to assess systemic risk in the interbank lending market, namely the network of financial interlinkages resulting from overnight loans between banks [12, 13]. Indeed, while interbank lending is crucial for banks to face fluctuating liquidity needs [14] and properly fuel the economy [15], the interbank market turns out to be rather fragile, as intra-system cash fluctuations alone have the potential to lead to systemic defaults [16], and exceptional liquidity shocks can lead to a complete market drought [2]. The latter scenario in particular characterized the period after the global financial crisis: banks held more liquid assets in anticipation of future expected losses and liquidity needs [17–19], and such a precautionary hoarding behavior caused a drastic increase of unsecured interbank borrowing rates for all but the shortest maturities [20]. The interbank market contraction was exacerbated even more by the massive liquidity injections from central banks, which instead of restoring interbank activity had the effect of replacing the market with the central banks balance sheets [21, 22]

The stream of literature on systemic risk analysis for interbank markets has focused on two main aspects: the network-based characterization of the topological structure of the market [13, 23–28], and the design of dynamics and metrics for the spread of financial distress over the network [1, 29–33]—in particular regarding shocks of liquidity [34–38]. In this work we add to this research field by proposing a modeling of liquidity-driven financial contagion in interbank networks through a compartment model similar to those commonly used in epidemiology [39, 40]. In particular, by assuming that liquidity shocks propagate as an epidemic disease over the market, we adapt the well-known SIR (*Susceptible-Infected-Removed*) model [41–43] to the specific context of interbank networks, and cast it as an EDB (*Exposed-Distressed-Bankrupted*) model. We simulate such a dynamical model on the Italian interbank network e-MID (electronic market for interbank deposits) [13, 25, 27, 28], analyzing liquidity contagion in relation with the structure and evolution of the network, and defining systemic risk through the resilience of individual banks and of the overall system to liquidity shocks.

In a nutshell, we show that the network topology of e-MID plays a fundamental and non-negligible role in the epidemics of liquidity distress, and that the total number of bank failures can assume very high values also when the initial shock is minimal. Importantly, systemic risk increases substantially at the onset of the global financial crisis, and goes back to pre-crisis values only after a highly unstable transient period. The probability to go bankrupt turns out to be higher for banks accounting for larger shares of the interbank network; however, the number of lenders of a bank can statistically explain riskiness more than the total amount of money borrowed, in line with the recent paradigm

* gbrandi@luiss.it

shift from "too big to fail" to "too interconnected to fail" [44]. We complement this analysis with a network-based study of e-MID, providing additional evidence that the market underwent significant changes due to the financial turmoil—with less banks participating to the market and executing fewer and lesser loan transactions. Liquidity hoarding had a considerable impact also on the underlying network structure: hub banks basically disappeared, the number of reciprocal and three-party contracts dropped, and—in spite of the reduced systemic risk—at the end the network lost its efficiency in terms money flow within banks.

The rest of the paper is structured as follows. Section II recalls basic features and network characterization of the e-MID dataset, and Section III presents a network analysis of the data. The EDB contagion model is defined in Section IV, and model simulation results are reported in Section V. Finally, Section VI presents an econometric study of simulation outcomes, and Section VII concludes.

II. E-MID DATA

The electronic Market for Interbank Deposits (e-MID) is a trading platform of unsecured money-market loans [45], that is unique in the Euro area for being screen-based and fully electronic. e-MID covers the entire domestic overnight deposit market in Italy, but is open to both Italian and foreign banks, and a significant share of all liquidity deposit in the Euro area is traded through the e-MID platform [46]. The dataset we have at our disposal consists of all the interbank transactions finalized on e-MID from January 1999 to September 2012. For each contract we have information about the amount exchanged, the date and time, the interest rate, the IDs of the lender and of the borrower banks, and the contract maturity [47].

Because of the data structure, e-MID (and interbank markets in general) is properly represented as a directed weighted network, where interbank loans constitute the direct exposures between banks and allow for the propagation of financial distress in the system. Here we focus on quarterly networks obtained by aggregating transactions over three months, as this time scale is enough to allow the emergence of complex interaction patterns [27]. To describe the network we employ the following notation. At quarter t, we have a system consisting of a set of N_t banks (the *nodes* of the network) and of L_t transactions among them—corresponding to the *links* connecting pairs of nodes. Transaction volumes are described by the $N_t \times N_t$ *weighted adjacency matrix* $\mathbf{W}(t)$, whose generic element $w_{ij}(t) \geq 0$ $(i, j = 1, \ldots, N_t)$ amounts to the overall loan that i granted to j (obtained by summing the single ON contracts resulting in a money flow from i to j). Analogously, the whole pattern of connections is described by the $N_t \times N_t$ *binary adjacency matrix* $\mathbf{A}(t)$, whose generic element $a_{ij}(t)$ equals 1 if a connection from node i to node j exists (*i.e.*, if bank j borrowed money from i during t so that $w_{ij}(t) > 0$), and 0 otherwise. Note that as in e-MID banks do not lend money to themselves, it is $a_{ii} = w_{ii} = 0\ \forall i$ by construction. The network built in this way is *directed*, meaning that in general $a_{ij}(t) \neq a_{ji}(t)$ and $w_{ij}(t) \neq w_{ji}(t)$ [25]. In the following we will restrict our analysis to the *weakly connected component* of the network, defined as the largest subnetwork in which any two nodes are connected to each other by a finite sequence of links (regardless of their direction). This restriction is particularly useful in the context of simulating epidemic cascades, as it eliminates the possibility that the infection cannot spread when starting from or stopping into sink nodes or isolated communities.

III. ANALYSIS OF NETWORK EVOLUTION

We now describe and analyze the network topology of e-MID, introducing a number of network quantities and showing the structural changes of the interbank market due to the global financial crisis.

A. Degree and Strength

For each bank i at quarter t, we define its *in-degree* $k_i^I(t) = \sum_{j \in N_t} a_{ji}(t)$ as the total number of incoming connections (that is, the number of banks that lent money to i during t). Similarly, its *out-degree* $k_i^O(t) = \sum_{j \in N_t} a_{ij}(t)$ is the total number of outgoing links (that is, the number of banks that borrowed money from i during t). The *reciprocal degree* $k_i^{\leftrightarrow}(t) = \sum_{j \in N_t} a_{ij}(t)a_{ji}(t)$ quantifies instead the number of banks that are at the same time borrowers and lenders of i. The overall number of trading partners is named *degree*, and is expressed as $k_i(t) = \sum_{j \in N_t}[a_{ij}(t) + a_{ji}(t) - a_{ij}(t)a_{ji}(t)] \equiv k_i^O(t) + k_i^I(t) - k_i^{\leftrightarrow}(t)$. Considering all banks, we can count the total number of links (that is, the number of bank pairs that finalized at least a transaction) during quarter t as $L_t = \sum_{ij} a_{ij}(t)$, and define the overall link *density* of the network as the number of realized links divided by the maximum number of possible links (*i.e.*, that of a fully connected network): $D_t = L_t/[N_t(N_t - 1)]$. Figure 1a shows that D_t remains quite stable

until the onset of the global financial crisis, and drops significantly thereafter as banks started to hoard liquidity and reduce the number of granted loans.

Concerning the distribution of banks connectivities, e-MID is characterized by a highly-skewed and long-tailed degree distribution $P(k)$, with the presence of a small number of "hub" banks with many connections and of a large number of banks with very few links [25]. Figure 1b shows the skewness coefficient of $P(k)$, which is indeed positive but features a decreasing trend before the crisis, and an increasing trend afterwards. The vanishing of the skewness coefficient during the crisis means that $P(k)$ loses its asymmetry during that period: degrees are distributed uniformly, and there are no hub banks in the network. In such a scenario, resulting from large banks drastically reducing their market participation, the network resilience to random failures of nodes drops [25].

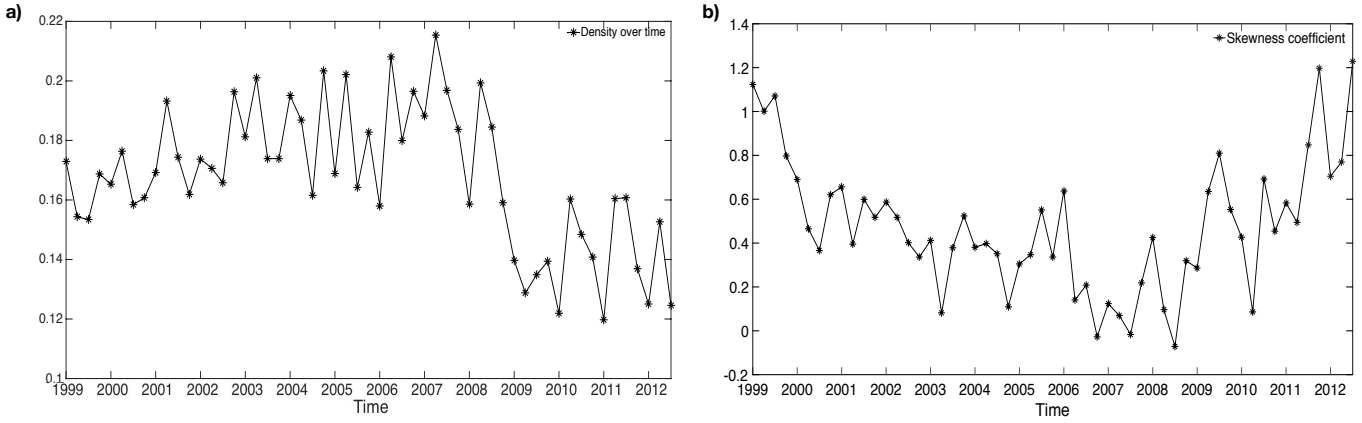

FIG. 1. **a) Network density in e-MID over time.** D_t remains stable until the crisis and then falls, as several banks diminished trading on e-MID from then on. **b) Skewness coefficient of the degree distribution in e-MID over time.** $P(k)$ is generally positively skewed, but the distribution becomes rather symmetric during the global financial crisis.

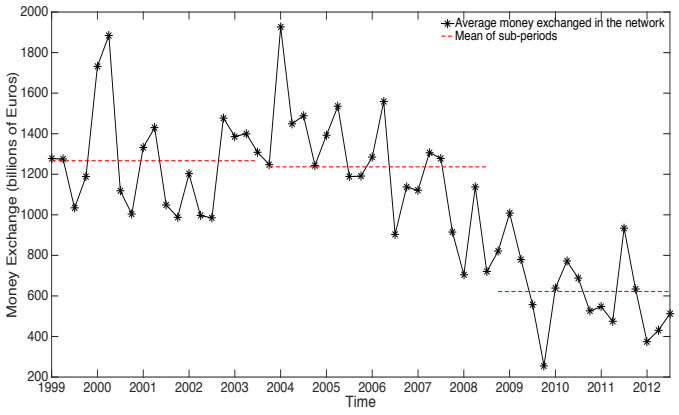

FIG. 2. **Average volume of money exchanged per bank over time.** Banks' participation to the market is stable until the crisis, and then drops consistently. According to a two-sample Kolmogorov-Smirnov test, the hypothesis that the average values before and after the crisis are derived from the same distribution is strongly rejected. On the contrary, when subdividing the pre-crisis period in two sub-periods, the hypothesis cannot be rejected: the trend is stable before the crisis.

Moving to the weighted structure of the network, we characterize each bank i by its *in-strength* $s_i^I(t) = \sum_{j \in N_t} w_{ji}(t)$ (the total amount of money borrowed from other banks), *out-strength* $s_i^O(t) = \sum_{j \in N_t} w_{ij}(t)$ (the total amount of money lent to other banks), and overall *strength* $s_i(t) = \sum_{j \in N_t} w_{ij}(t) + w_{ji}(t) \equiv s_i^O(t) + s_i^I(t)$ (the total amount of money exchanged by that bank). Similarly to the number of links, the total volume of trades at quarter t is defined as $V_t = \sum_{ij} w_{ij}(t)$. Figure 2 shows that the average volume of money exchanged per bank (V_t/N_t) drops during the global financial crisis: again, during turmoils banks hand out less loans as worries of counterparty creditworthiness

prevail over the increasing possible gains due to interest rate bursts [48, 49]. Average traded volumes remain low also after the crisis, supposedly because of the difficulties in re-building trust between banks.

B. Core-periphery structure

At the quarterly aggregation level, e-MID is characterized by a *core-periphery structure*: hub banks (the *core*) are highly connected among themselves, whereas, the other leaf banks (the *periphery*) are connected mostly to the core, and very few links exist within the periphery [28] [50]. Here we resort to the method by Craig and Von Peter [51] to identify core and periphery banks, and employ the obtained partition in the analysis of overall network properties presented in Figure 3. In particular, Figure 3a shows the decreasing trend of the number of *active banks* N_t, namely the number of banks that appear at least in one e-MID transaction at quarter t. Figures 3b and 3c respectively show that also the number of connections L_t and the volume exchanged V_t decrease over time, whatever these quantities are computed within the core, within the periphery, and between core and periphery. Note that the decrease of L_t and V_t is only partially explained by the fewer number of active banks N_t (in fact, V_t/N_t is almost constant before the crisis, see Figure 2). In this respect, while precautionary motives can be responsible for having less active banks since the onset of the crisis, mergers and acquisitions could have played a significant role beforehand.

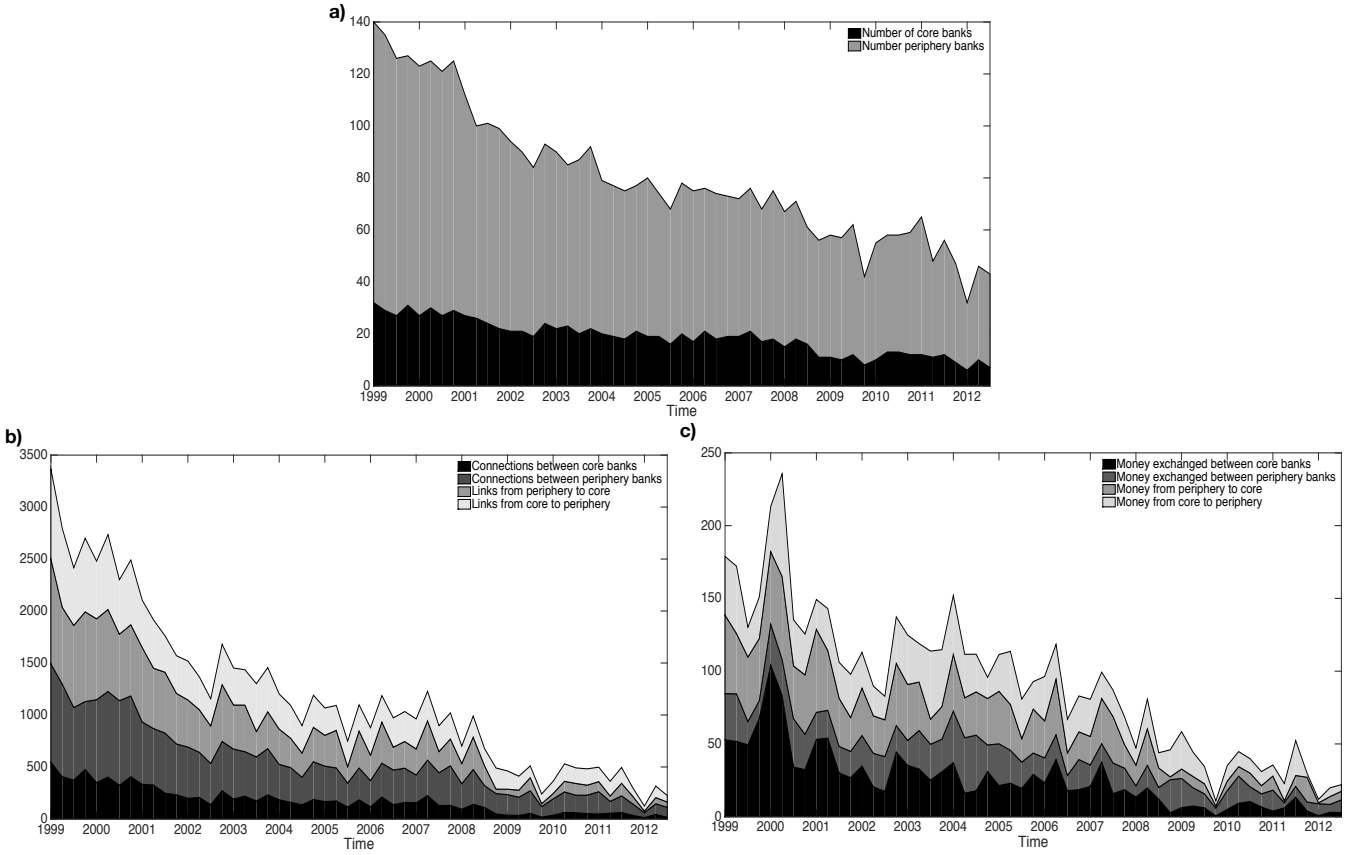

FIG. 3. **Core-periphery network analysis over time.** Stacked histograms for: a) Number of active banks N_t; b) Number of links between active banks L_t; c) Volume of money exchanged V_t.

C. Reciprocity, clustering and efficiency

We now turn our attention to network metrics related to the local structure of connections, and in particular to preferential lending between banks. *Reciprocity* is defined as the the number of bidirectional links over the total

number of links in the network: $r_t = L_t^{\leftrightarrow}/L_t$, where $L_t^{\leftrightarrow} = \sum_{i<j} a_{ij}(t)a_{ji}(t)$. *Clustering* measures the probability that two banks have a common trading counterpart, and is defined as the average ratio between the number of link triangles to the total possible number of such triangles. In its simplest undirected version, the clustering coefficient is defined as $c_t = \sum_i \{[\sum_{jh} u_{ij}(t)\, u_{ih}(t)\, u_{jh}(t)]/[k_i^2(t) - k_i(t)]\}/N_t$, where $u_{ij}(t) = a_{ij}(t) + a_{ji}(t) - a_{ij}(t)a_{ji}(t)$ [52]. *Efficiency* instead measures how well liquidity (or information in general) is exchanged and flows within the network, and is defined as the average of the inverses of the shortest path length between node pairs: $e_t = \sum_{ij} d_{ij}^{-1}(t)/[N_t(N_t-1)]$, where d_{ij} is the length (in number of links) of the shortest path from node i to node j [53]. The temporal evolution of these quantities is reported in Figure 4. Again we observe a stable behavior that changes abruptly during the financial crisis, and previous stationary values are not recovered even years later. This indicates that banks behavior due to the crisis (liquidity hoarding and distrust for counterparty creditworthiness) caused a structural break in the market, so that recovering the pre-crisis configuration may require a strong exogenous intervention and system-level modifications.

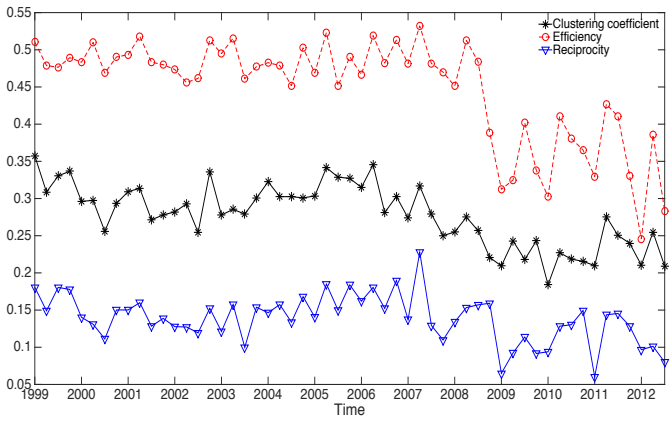

FIG. 4. **Reciprocity, clustering and efficiency coefficients over time.** The drop of efficiency at the global financial crisis is particularly evident, and basically marks the interbank market freeze [22].

IV. LIQUIDITY-DRIVEN CONTAGION MODEL

We now present the EDB dynamical model of liquidity contagion in interbank networks. We start by briefly describing the standard SIR model used in epidemiology, and then proceed step by step to its adaptation for interbank lending markets.

A. The Susceptible-Infected-Removed model

The SIR model is a deterministic compartment model introduced by Kermack and McKendrick [41]. It considers a fixed population of individuals, each of which can be in one of three possible states: susceptible ($\mathcal{S}$), infected ($\mathcal{I}$) and removed (or recovered) ($\mathcal{R}$). The model dynamics then set the transition probabilities between the compartments: infected individuals can spread the infection to susceptible ones with a given probability λ; on the other hand, infected individuals are removed from the system at a rate μ. The dynamical flow of SIR model is thus $\mathcal{S} \to \mathcal{I} \to \mathcal{R}$, and the model equation for a well-mixed population are:

$$\frac{ds}{dt} = -\lambda si \qquad \frac{di}{dt} = \lambda si - \mu i \qquad \frac{dr}{dt} = \mu i$$

where s, i and r are the densities of susceptible, infected and removed individuals, respectively, such that $s+i+r = 1$. This model can be implemented on any network structure by restricting the $\mathcal{S} \to \mathcal{I}$ transitions to realized links: infected individuals can only transmit the disease to their susceptible neighbors.

The SIR model builds on several simplifying assumptions such as that of a link-independent infection rate and a node-independent removal rate, which can be appropriate for humans having similar immune responses but fails in

other contexts where contagion channels can be of very different extent. A recent attempt to extend the SIR model to the more realistic scenario of weighted directed networks is provided by Chu *et al.* [42]: they still assume a constant removal rate μ, but the infection probability becomes dependent on link weights. In particular, the probability that the infection spreads from an infected individual i to her susceptible neighbor j reads $\lambda_{ij} = \lambda k_i^O w_{ij}/s_i^O$, meaning that outgoing links with larger weights become preferential contagion channels.

B. The Exposed-Distressed-Bankrupted model

Building on the SIR model and its adaptation to weighted directed network, we now assemble our model for liquidity-driven financial contagion: the *Exposed-Distressed-Bankrupted* model (EDB). We start by briefly recalling the features of the interbank lending market, which is the context we want to describe. The market allows banks to face liquidity fluctuations and meet reserve requirements at the end of the trading day, as banks temporarily short on liquidity borrow money from other banks having excess liquidity. The majority of contracts within the market has overnight duration, meaning that they are placed, and shortly after resolved and rolled-over—as banks may need additional liquidity to refinance their activities. The system is thus subject to *roll-over risk*: banks debt that is about to mature needs to be replaced by a new debt, yet if because of a crisis the market offer for fundings drops, banks may fail to meet their short-term obligations and be forced to enter bankruptcy, or to sell their illiquid assets resulting in potentially large losses during fire sales [2]. These spillovers create the incentive to hoard liquidity [19], which can in turn induce another wave of liquidity shocks, activating a spiral that can lead the interbank market to freeze completely [20, 22].

Once the liquidity risk dynamics of the market has been set down, we can formulate the analytics of the EDB model. We basically assume that liquidity losses propagate as an epidemic disease over the market: funding losses experienced by a bank imply a decreasing capability to lend money to the market (even if no default has occurred), which in turn may cause liquidity shortages for other banks unable to borrow all the liquidity they need. A simple way to translate these concepts into a dynamical system is the following. Similarly to SIR, each bank can be in one of three states: exposed ($\mathcal{E}$), distressed ($\mathcal{D}$) and bankrupted ($\mathcal{B}$). Exposed banks are healthy in the sense that they get full liquidity supply from the market, but are subject to financial contagion from both distressed and defaulted banks. If contagion occurs by losses of liquidity provision, an exposed bank becomes distressed. Finally, when liquidity losses become overwhelming, a distressed bank eventually fails and switches to the bankrupted state.

The "infection" probability, *i.e.*, the probability that a distressed or defaulted bank i transmits a liquidity shock to an exposed bank j, depends on the transaction volume between the two institutions. In particular, we assume that the higher the loan i granted to j (w_{ij}), the higher the probability that i (which is short of liquidity) cuts the funding, resulting in a liquidity loss for j. In general we assume:

$$\lambda_{ij} = \varphi\left(\frac{w_{ij}}{s_i^O}\right) \tag{1}$$

where $\varphi(\cdot)$ is an appropriately chosen function that obeys $\varphi(0) = 0$ and $\varphi(1) = 1$ (see below) [54]. The role of the normalization factor $s_i^O = \sum_j w_{ij}$ is to have $\lambda_{ij} \equiv 1$ in the case of a distressed or defaulted bank i lending money only to one exposed bank j.

On the other hand, the "bankruptcy" probability for distressed bank i is assumed to be:

$$\mu_i = \psi\left(\frac{\sum_{j\in N\setminus\mathcal{E}} w_{ji}}{\sum_j w_{ji}}\right) \equiv \psi\left(\frac{\tilde{s}_i^I}{s_i^I}\right) \tag{2}$$

where $N \setminus \mathcal{E}$ is the set of distressed and bankrupted banks, $\tilde{s}_i^I$ is the in-strength of i restricted to this set, and $\psi(\cdot)$ is another appropriately chosen function that obeys $\psi(0) = 0$ and $\psi(1) = 1$ (see below). The ratio $\tilde{s}_i^I/s_i^I$ is precisely the proportion of liquidity bank i needs that was previously obtained from unhealthy institutions: a bank goes bankrupt if this proportion is too high, given the assumption that banks cannot efficiently and immediately reallocate their asset and liabilities to absorb the distress. Indeed, bank i gets no liquidity at all if each of its lenders is in the distressed or bankrupted state, going bankrupt with probability 1.

While we leave the discussion on how to set the functions $\varphi(\cdot)$ and $\psi(\cdot)$ to the next section [55], we conclude here by stressing that, differently from the SIR model or the one by Chu *et al.* [42], in our setting the infection propagates from both distressed and bankrupted banks, who fail to provide liquidity to the market. Additionally, financial institutions can bear diverse level of losses (up to s^I): some are more resilient to liquidity shocks than others, so that a moderate level of distress can be absorbed easily by large banks, but can be lethal for small banks.

V. SIMULATION RESULTS

In this section we present results of agent-based simulations for the EDB model on the network topology of e-MID. The numerical program is designed as follows. Initially, all banks are healthy and thus belong to the exposed state $\mathcal{E}$. Then, an exogenous liquidity shock hits a set of randomly chosen banks, which are thus put into the distress state $\mathcal{D}$ We use different dimensions for this set: 1%, 5%, 10% and 20% of total banks. The dynamics then proceeds in discrete time steps, for each of which:

- Distressed and bankrupted banks can infect their exposed debtor banks, with probability given by eq. (1). If infected, an exposed bank switches to the distressed state (and can thus propagate liquidity shocks in the next step).
- After the propagation of the infection, distressed banks can go bankrupt at a rate given by eq. (2).

The simulation stops when there are no distressed banks left in the market, or if a maximum number of steps is reached [56]. We then compute the fraction of bankrupted banks in the market, and average it over 5000 independent realizations of the system to have a proxy for systemic risk. Individual risk of banks is instead assessed through their default frequencies over these realizations. For our analysis, we implement three different economic scenarios by changing the shape of the functions $\varphi(\cdot)$ and $\psi(\cdot)$:

1. LC-LD (linear contagion – linear default). The infection probability is linearly proportional to the exposure between banks, and the default probability is linearly proportional to the ratio between the faced liquidity shortage and the overall financial needs of a bank, resulting into linear expressions $\varphi(x) = \psi(x) = x$.
2. LC-NLD (linear contagion – nonlinear default). The infection probability is linear $\varphi(x) = x$, but the default probability is a nonlinear function characterized by a threshold γ, so that $\psi(x) \simeq x$ for $x < \gamma$ and $\psi(x) \simeq 1$ for $x \geq \gamma$. The latter choice reflects a situation in which banks with little liquidity shortages have easy access to funding (from external channels such as central banks injecting liquidity in the market) and are thus less likely to go bankrupt, whereas, the default probability jumps when liquidity shortages surpass a threshold, as access to external funding is denied for exceeding regulatory constraints. Here we use a regularized incomplete beta function $\psi(x) = I_x(5, 20)$, which results in an implicit threshold at $\gamma \simeq 17\%$.
3. NLC-NLD (nonlinear contagion – nonlinear default). The infection probability grows more than linearly with the exposure, mimicking a liquidity hoarding tendency for distressed banks which puts more liquidity pressure on their counterparties, whereas, the default probability is kept nonlinear. Here we use again a regularized incomplete beta function $\varphi(x) = I_x(1, 2)$.

Figure 5 shows simulation results for different initial densities of distressed banks and for the three economic scenarios presented above. The first evident observation is that the temporal trends of systemic risk for the three economies are highly correlated, and basically differ just for a vertical shift. This suggests that the network topology (which is the same in the three settings) plays a fundamental role in the epidemic diffusion. The overall level of systemic risk in the system can assume worrying high values (from about 40% up to almost 90% also when the initial density of distressed bank is just 1%), pointing to the importance of considering network effects when assessing the system resilience to liquidity shocks. Naturally, the resulting systemic risk increases for higher initial densities of distressed banks, but the relationship between these two variables is nonlinear: the number of bankruptcies grows only by a few percentage points (on average, 6%, 12% and 19%) for multiples of the initial density (5, 10 and 20 times, respectively), indicating that liquidity losses in the market can saturate even for a small initial distress. In any event, the most interesting feature of Figure 5 is that the number of bankrupted banks increases substantially at the onset of the global financial crisis, and goes back to pre-crisis values only after a transient period characterized by heavy fluctuations—signaling a phase of high instability for the interbank market. The drop of systemic risk after the crisis can be indeed attributed to precautionary banks behavior, as demonstrated by the decreasing number of banks participating to the market and the even more decreasing number and volume of transactions (see Figure 3). Yet, the reduced network density is not enough to explain the recovered resilience, and the structural changes of the market topology have been determinant in this sense. In order to prove this statement, we perform a statistical test by measuring systemic risk as simulated on an ensemble of null networks, *i.e.*, random networks with the same density, degree sequence and strength sequence of e-MID network snapshots after the crisis [57, 58]. Using a two-sample Kolmogorov-Smirnov test, the null hypothesis that the two risk measures come from independent random samples of the same normal distribution is rejected at the 0.1% confidence level.

Note that an apparent contradiction to the above discussed relation between liquidity hoarding and systemic risk emerges by observing the remarkably higher number of defaults in the third scenario, where a sort of hoarding

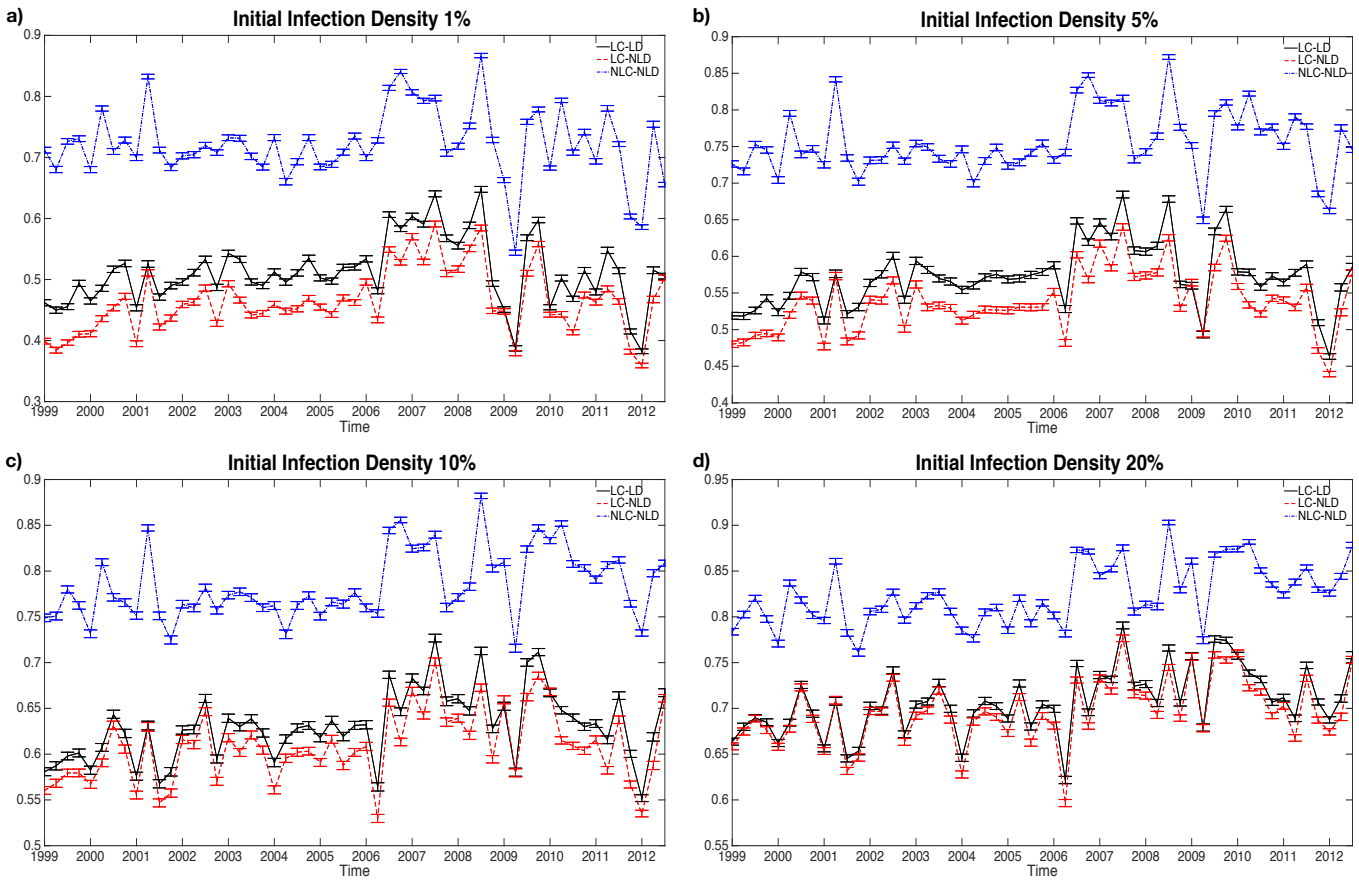

FIG. 5. **Average ratio of bankrupted banks at the end of simulations, for various initial densities of distressed banks.** The number of defaults reaches its maximum value just before the beginning of the financial crisis, and then drops as a result of banks precautionary behavior.

tendency enters in the contagion dynamics: the probability that banks cut their liquidity provision is higher than in the other economies, significantly enhancing the spreading of the liquidity disease. What happens here is that a liquidity hoarding behavior simulated on a given market configuration has the effect of increasing liquidity risk. However, if banks actually hoard liquidity then the realized market structure changes, and the new configuration is more resilient to liquidity shocks, mainly because is deprived from its functionality of liquidity provider to banks.

Besides assessing systemic risk through the number of bankrupted banks, we can measure the overall liquidity loss in the market by accounting for the size of defaulted banks. We thus compute the ratio between the amount of liquidity originally granted by bankrupted banks and the overall starting market liquidity, that is $\sum_{i\in\mathcal{B}} s_i^O / \sum_i s_i^O$. Figure 6 shows that the ratio of liquidity loss is remarkably high over the whole time span of the data, suggesting again that a small initial shock can lead to severe systemic losses. Importantly, the monetary damage is much higher than the risk metric given by the percentage of bankruptcies, indicating that banks accounting for larger shares of the interbank network, *i.e.*, banks belonging to the network core [51], are actually more likely to default.

We conclude the section by studying which network features make a bank more vulnerable to liquidity shocks. To do so we evaluate, for each quarter, the correlation coefficient between the in/out-degree and in-out/strength sequences of banks and their individual risk (assessed by the frequency of default events). Figure 7 shows that the liquidity riskiness of a bank is highly correlated with its in-degree (that is, the number of lenders) and in-strength (the total amount of money borrowed): banks that rely more on the market to fund their activities are, as expected, more vulnerable to liquidity shocks.

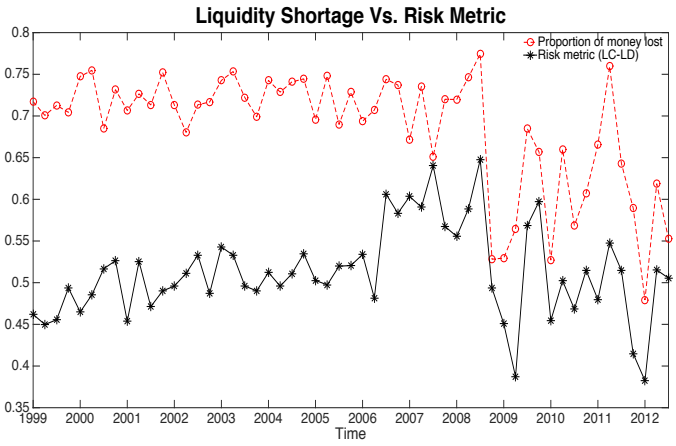

FIG. 6. **Relative liquidity loss and systemic risk given by the ratio of bankrupted banks.** Results refer to the first economic scenario (LC-LD) and to a density of initially distressed banks equal to 1%.

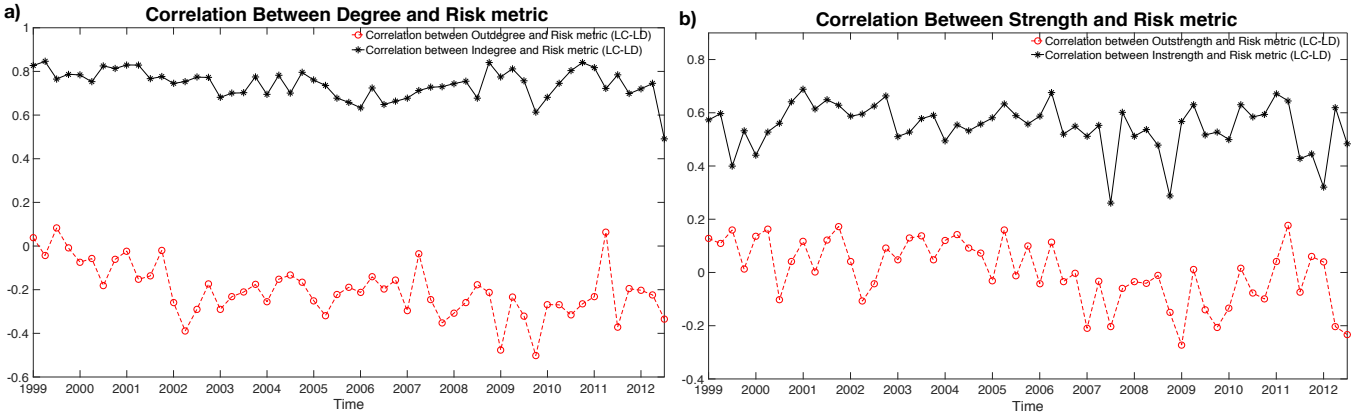
a)
Correlation Between Degree and Risk metric
Correlation between Outdegree and Risk metric (LC-LD)
Correlation between Indegree and Risk metric (LC-LD)
Time
b)
Correlation Between Strength and Risk metric
Correlation between Outstrength and Risk metric (LC-LD)
Correlation between Instrength and Risk metric (LC-LD)
Time

FIG. 7. **Time evolution of the correlation coefficients between banks network features and individual risk.** a) correlation between in/out-degree and risk metric; b) correlation between in/out-strength and risk metric.

VI. ECONOMETRIC ANALYSIS

In this section we run a statistical exercise in order to discern the contribution of different network features of a bank on its liquidity riskiness. Among the various features that may affect the likelihood of bank failure, we focus on the following two set of quantities to be used as regressors in our analysis:

- *binary features*: in-degree, out-degree, binary-clustering, coreness and betweenness;
- *weighted features*: in-strength, out-strength, weighted-clustering, coreness and betweenness.

In the above lists of quantities, degrees and strengths are defined in section 3.1; binary-clustering is defined in section 3.3, and weighted-clustering is obtained with the same expression of its binary counterpart by using $u_{ij}(t) = w_{ij}(t) + w_{ji}(t)$ [52]; coreness is a dummy variable taking the value of 1 if the considered bank is in the core and 0 otherwise [51]; betweenness is the fraction of all the shortest paths in the network that pass through the considered bank [59]. All these quantities are measures of nodes centrality (or importance) in the network. Indicating as $x_i^m(t)$ the value of variable m for bank i at time t, our benchmark regression reads:

$$y_i(t) = \omega_i + \eta(t) + \sum_m \alpha_m x_i^m(t) + \Theta_t \sum_m \beta_m x_i^m(t) + \zeta\Theta_t + \varepsilon_i(t), \tag{3}$$

where $y_i(t)$ is the dependent variable, namely the default frequency in the EDB model observed for each individual bank i at date t. In the above expression, we account for unobserved heterogeneity at bank level through the coefficient

TABLE I. **Regression results for independent variables given by binary network features of banks.**

	Infection Probability			
	1%	5%	10%	20%
α_coreness	0.044***	0.043***	0.040***	0.034***
	(0.003)	(0.003)	(0.003)	(0.003)
α_betweenness	7.162***	6.370***	5.267***	3.986***
	(1.257)	(1.218)	(1.158)	(1.044)
α_binary-clustering	0.095	-1.003	-1.219	-1.594
	(3.950)	(3.828)	(3.638)	(3.282)
α_in-degree	0.775***	0.734***	0.681***	0.582***
	(0.037)	(0.036)	(0.034)	(0.031)
α_out-degree	-1.609***	-1.535***	-1.409***	-1.185***
	(0.038)	(0.036)	(0.035)	(0.031)
β_coreness	0.007	0.015	0.018	0.019*
	(0.011)	(0.011)	(0.010)	(0.009)
β_betweenness	-7.047*	-5.967*	-4.554	-2.369
	(2.766)	(2.681)	(2.548)	(2.299)
β_binary-clustering	15.608	14.351	13.196	12.133
	(8.798)	(8.527)	(8.104)	(7.310)
β_in-degree	1.600***	1.558***	1.398***	1.010***
	(0.161)	(0.156)	(0.148)	(0.134)
β_out-degree	-1.581***	-1.671***	-1.599***	-1.277***
	(0.143)	(0.139)	(0.132)	(0.119)
ζ	-15.824***	-12.504***	-8.805**	-4.208
	(2.979)	(2.887)	(2.744)	(2.475)
η	46.173***	52.378***	57.965***	65.911***
	(1.562)	(1.513)	(1.438)	(1.298)
N	4387	4387	4387	4387
adj. R^2	0.358	0.355	0.341	0.309

Standard errors in parentheses

* $p < 0.05$, ** $p < 0.01$, *** $p < 0.001$

TABLE II. **Regression results for independent variables given by weighted network features of banks.**

	Infection Probability			
	1%	5%	10%	20%
α_coreness	0.039***	0.038***	0.036***	0.032***
	(0.003)	(0.003)	(0.003)	(0.003)
α_betweenness	6.921***	6.318***	5.529***	4.516***
	(1.400)	(1.359)	(1.285)	(1.141)
α_weighted-clustering	0.019*	0.018*	0.017*	0.014*
	(0.009)	(0.008)	(0.008)	(0.007)
α_in-strength	0.003***	0.003***	0.002***	0.002***
	(0.000)	(0.000)	(0.000)	(0.000)
α_out-strength	-0.003***	-0.003***	-0.002***	-0.002***
	(0.000)	(0.000)	(0.000)	(0.000)
β_coreness	0.047***	0.050***	0.048***	0.039***
	(0.011)	(0.011)	(0.010)	(0.009)
β_betweenness	-4.718	-4.715	-4.311	-3.276
	(2.900)	(2.815)	(2.661)	(2.364)
β_weighted-clustering	0.072	0.082	0.077	0.052
	(0.086)	(0.083)	(0.079)	(0.070)
β_in-strength	0.000	0.001	0.001	0.001
	(0.001)	(0.001)	(0.001)	(0.001)
β_out-strength	-0.004***	-0.004***	-0.004***	-0.003***
	(0.001)	(0.001)	(0.001)	(0.001)
ζ	-0.441	1.470	3.207*	4.794***
	(1.443)	(1.400)	(1.324)	(1.176)
η	45.153***	51.102***	57.035***	65.287***
	(0.610)	(0.592)	(0.560)	(0.497)
N	4387	4387	4387	4387
adj. R^2	0.127	0.119	0.110	0.095

Standard errors in parentheses

* $p < 0.05$, ** $p < 0.01$, *** $p < 0.001$

ω_i, encompassing a variety of time-invariant factors such as bank location, institutional features of the country where it is based, ownership, and so on. On the other hand, $\eta(t)$ accounts for generic temporal effects such as aggregate shocks hitting the market at time t. We also introduce N_t discontinuities through the dummy variable Θ_t taking on the value 0 before the global financial crisis and 1 afterwards, in order to capture any change of variables due to the crisis. Overall, the sets of regression coefficients we are interested in are $\{\alpha_m\}$, indicating whether feature m explains the variability of default frequencies, and $\{\beta_m\}$, showing how the effect of feature m changes after the crisis.

Tables I and II show regression results for the set of binary and weighted variables, respectively [60]. In both cases, we consider an initial density of distressed banks equal to 1%, 5%, 10% and 20% (corresponding to the different table columns). As a general observation, we see that bank network features, *i.e.*, the topology of the network, plays an increasing significant role for a decreasing initial density of distressed banks. This means that network effects are important especially at the onset of a financial turmoil period. We then observe that betweenness and coreness do influence the default frequency, while clustering is the only metric that does not. Concerning the binary features reported in Table I, we see that the number of lenders of a given bank covariates positively with that bank's default frequency, whereas, the number of borrowers for that bank does it negatively. Table II then shows that also the total borrowing and lending are significant variables, however their effect is negligible compared to that of their binary counterparts. Finally, concerning the impact of variables after the crisis, we basically find a statistically null effect for betweenness, coreness and clustering. Discontinuities are instead observed for banks connectivities, with in-degree doubling its effect after the crisis. The impact of the crisis itself, represented by the coefficient ζ, is remarkable for the binary set of regressors: default frequencies drops after the crisis due to the diminished trades between banks (liquidity hoarding).

Overall, the goodness of the two regressions in term of adjusted R^2 indicates that the binary features can explain the variability of the dependent variable three times more than the weighted features. We can thus conclude that betweenness and in/out-degree are more explanatory for systemic risk than the other variables, in line with the recent paradigm shift from "too big to fail" to "too interconnected to fail" [44].

VII. CONCLUSIONS

In this work we have addressed the issue of systemic risk in interbank markets due to liquidity shortcomings. Using transaction data from the Italian electronic market for interbank deposits (e-MID), we have analyzed the interbank network structure, and studied its resilience to liquidity shocks through the introduction of the *Exposed-Distressed-Bankrupted* (EDB) model—simulating an epidemic dynamics of liquidity disease within the market. We found that the 2007/2008 global financial crisis had a significant impact on the network topology: liquidity hoarding policies and worries of counterparty creditworthiness resulted not only in a poorer interbank market in terms of active participants and density/extent of transactions, but also in structural changes of the market itself such as the disappearance of hub banks and preferential lending channels—which ultimately led the interbank network to become less efficient in terms of monetary flow between banks. Indeed, results of the EDB model show that systemic risk was maximal at the onset of the global financial crisis, and the subsequent financial burst forced banks to change their strategic behavior to adapt to the new harsher environment, ultimately lowering risk but depriving the market from its functionalities. We also point out that dynamics of liquidity shocks reverberation on the interbank network are extremely important to consider in stress-test scenarios, as the overall losses in the system can be severe also for weak initial shocks. The failure probability turns out to be enhanced for banks that rely heavily on the market for liquidity provision, especially in terms of number of borrowers: a high diversification of funding channels usually minimize roll-over risk for low level of financial distress, but during crisis periods it increases the probability to be hit by a liquidity shock.

The EDB model we implement in this work can be further generalized by acting on the infection and default probabilities, which can be modified to include exogenous spillovers. For instance, the default rate could be made depend on depositors withdraws, or include bailout mechanisms that bring a bank back to the exposed state. Finally note that the EDB model is implemented without considering the detailed balance sheet positions of banks, to which we do not have access through e-MID data. While such a simplification is not crucial when studying qualitatively the financial (in)stability of the market in relation with its network topological structure, the model is open to account for banks balance sheet information, in order to properly assess the real extent of liquidity-driven systemic risk in interbank markets.

ACKNOWLEDGMENTS

We thank Alessandro Belmonte for useful discussions. Giulio Cimini and Riccardo Di Clemente acknowledge support from project GROWTHCOM (FP7-ICT, n. 611272). Giulio Cimini also acknowledges support from projects

MULTIPLEX (FP7-ICT, n. 317532) and DOLFINS (H2020-EU.1.2.2., n. 640772). The funders had no role in study design, data collection and analysis, decision to publish, or preparation of the manuscript.

[1] J. A. Chan-Lau, M. Espinosa, K. Giesecke, and J. A. Solé, *Assessing the Systemic Implications of Financial Linkages*, IMF Global Financial Stability Report 2 (2009).
[2] M. K. Brunnermeier, Journal of Economic Perspectives **23**, 77 (2009).
[3] S. Battiston, G. Caldarelli, R. May, T. Roukny, and J. E. Stiglitz, Columbia Business School Research Paper (2015).
[4] S. Battiston, J. D. Farmer, A. Flache, D. Garlaschelli, A. G. Haldane, H. Heesterbeek, C. Hommes, C. Jaeger, R. May, and M. Scheffer, Science **351**, 818 (2016).
[5] F. Allen and D. Gale, Journal of Political Economy **108**, 1 (2000).
[6] P. Gai, A. Haldane, and S. Kapadia, Journal of Monetary Economics **58**, 453 (2011).
[7] F. Caccioli, M. Shrestha, C. Moore, and J. D. Farmer, Journal of Banking & Finance **46**, 233 (2014).
[8] D. Acemoglu, A. Ozdaglar, and A. Tahbaz-Salehi, American Economic Review **105**, 564 (2015).
[9] R. Greenwood, A. Landier, and D. Thesmar, Journal of Financial Economics **115**, 471 (2015).
[10] S. Gualdi, G. Cimini, K. Primicerio, R. D. Clemente, and D. Challet, arXiv:1603.05914 (2016).
[11] P. Barucca, M. Bardoscia, F. Caccioli, M. D'Errico, G. Visentin, S. Battiston, and G. Caldarelli, arXiv:1606.05164 (2016).
[12] J.-C. Rochet and J. Tirole, Journal of Money, Credit and Banking **28**, 733 (1996).
[13] G. Iori, S. Jafarey, and F. G. Padilla, Journal of Economic Behavior & Organization **61**, 525 (2006).
[14] F. Allen, A. Hryckiewicz, O. Kowalewski, and G. Tümer-Alkan, Journal of Financial Stability **15**, 112 (2014).
[15] G. Gabbi, G. Iori, S. Jafarey, and J. Porter, Journal of Economic Dynamics & Control **50**, 117 (2015).
[16] P. Smaga, M. Wiliński, P. Ochnicki, P. Arendarski, and T. Gubiec, arXiv:1603.05142 (2016).
[17] J. W. van den End, M. Tabbae, *et al.*, *When Liquidity Risk Becomes a Macro-Prudential Issue: Empirical Evidence of Bank Behaviour*, DNB Working Paper Series 230 (2009).
[18] P. Gai and S. Kapadia, in *Proceedings of the Royal Society A*, Vol. 466 (2010) p. 439.
[19] J. M. Berrospide, *Bank Liquidity Hoarding and the Financial Crisis: An Empirical Evaluation*, FEDS Working Paper Series 03 (2013).
[20] V. V. Acharya and D. Skeie, Journal of Monetary Economics **58**, 436 (2011).
[21] F. Heider, M. Hoerova, and C. Holthausen, *Liquidity Hoarding and Interbank Market Spreads: The Role of Counterparty Risk*, ECB Working Paper Series 1126 (2009).
[22] S. Gabrieli and G. Co-Pierre, *A Network View on Interbank Market Freezes*, Banque de France Working Paper Series 531 (2014).
[23] S. Wells, Financial Stability Review **13**, 175 (2002).
[24] M. Boss, H. Elsinger, M. Summer, and S. Thurner, Quantitative Finance **4**, 677 (2004).
[25] G. Iori, G. De Masi, O. V. Precup, G. Gabbi, and G. Caldarelli, Journal of Economic Dynamics & Control **32**, 259 (2008).
[26] J. F. Cocco, F. J. Gomes, and N. C. Martins, Journal of Financial Intermediation **18**, 24 (2009).
[27] K. Finger, D. Fricke, and T. Lux, Computational Management Science **10**, 187 (2013).
[28] D. Fricke and T. Lux, Computational Economics **45**, 359 (2015).
[29] L. Eisenberg and T. H. Noe, Management Science **47**, 236 (2001).
[30] H. Elsinger, A. Lehar, and M. Summer, Management Science **52**, 1301 (2006).
[31] E. Nier, J. Yang, T. Yorulmazer, and A. Alentorn, Journal of Economic Dynamics & Control **31**, 2033 (2007).
[32] A. Krause and S. Giansante, Journal of Economic Behavior & Organization **83**, 583 (2012).
[33] S. Battiston, M. Puliga, R. Kaushik, P. Tasca, and G. Caldarelli, Scientific Reports **2**, 541 (2012).
[34] R. Cifuentes, G. Ferrucci, and H. S. Shin, Journal of the European Economic Association **3**, 556 (2005).
[35] D. W. Diamond and R. G. Rajan, *Fear of Fire Sales and the Credit Freeze*, NBER Working Paper Series 14925 (2009).
[36] S. Kapadia, M. Drehmann, J. Elliott, and G. Sterne, "Liquidity risk, cash flow constraints, and systemic feedbacks," in *Quantifying Systemic Risk* (University of Chicago Press, 2012) pp. 29–61.
[37] T. R. Hurd, D. Cellai, S. Melnik, and Q. Shao, arXiv:1310.6873 (2013).
[38] G. Cimini and M. Serri, PLoS ONE **11**, 1 (2016).
[39] M. J. Keeling and K. T. Eames, Journal of the Royal Society Interface **2**, 295 (2005).
[40] R. Pastor-Satorras, C. Castellano, P. Van Mieghem, and A. Vespignani, Review of Modern Physics **87**, 925 (2015).
[41] W. O. Kermack and A. G. McKendrick, in *Proceedings of the Royal Society of London A: Mathematical, Physical and Engineering Sciences*, Vol. 115 (The Royal Society, 1927) pp. 700–721.
[42] X. Chu, Z. Zhang, J. Guan, and S. Zhou, Physica A: Statistical Mechanics and its Applications **390**, 471 (2011).
[43] Y. Sun, C. Liu, C.-X. Zhang, and Z.-K. Zhang, Physics Letters A **378**, 635 (2014).
[44] A.-C. Hüser, *Too Interconnected to Fail: A Survey of the Interbank Networks Literature*, SAFE Working Paper 91 (2015).
[45] An anonymous and collateralized segment of e-MID (New MIC) was introduced in February 2009 with the aim of improving the liquidity distribution within the euro area [61].
[46] R. Beaupain and A. Durré, *The Interday and Intraday Patterns of the Overnight Market: Evidence from an Electronic Platform*, ECB Working Paper Series 0988 (2008).

[47] Transactions can be ON (overnight), ONL (overnight long), TN (tomorrow next), TNL (tomorrow next long), SN (spot next), SNL (spot next long), 1W (one week), 1WL (one week long), 2W (two weeks), 3W (three weeks), 1M (one month), 2M (two months), 3M (three months), 4M (four months), 5M (five months), 6M (six months), 7M (seven months), 8M (eight months), 9M (nine month), 10M (ten months), 11M (eleven months), 1Y (one year). In this paper we use only overnight transactions, which represent the vast majority of trades (approximately 90%).
[48] B. Lyons, CPI Journal **5**, 2 (2009).
[49] B. De Meester, *Liberalization of Trade in Banking Services: An International and European Perspective* (Cambridge University Press, 2014).
[50] At aggregation levels shorter than one week, the network is instead better characterized by a bipartite (or *bow-tie*) structure, with some banks that preferentially lend and other banks that preferentially borrow [62].
[51] B. Craig and G. Von Peter, Journal of Financial Intermediation **23**, 322 (2014).
[52] G. Fagiolo, Physical Review E **76**, 026107 (2007).
[53] V. Latora and M. Marchiori, Physical Review Letters **87**, 198701 (2001).
[54] For a linear $\varphi(\cdot)$, eq. (1) is analogous to the expression used in [42]—apart from a pre-factor and the dependence on the out-degree of the source node.
[55] The model can be further extended by adding a stochastic noise $\epsilon \sim U(0, \nu)$ to the infection and default probabilities: $\varphi(x) \to \varphi(x) + \epsilon$ and $\psi(x) \to \psi(x) + \epsilon$. Such a noise simulates instantaneous exogenous shocks, generated for instance by private depositors withdraws. The upper bound of the shock $\nu > 0$ can be calibrated as the maximum amount of withdraw allowed by a bank under distress. For the sake of simplicity, in this work we do not consider this possibility.
[56] The stop condition of no distressed banks left in the market means that, from then on, no more defaults can occur—unless an exposed bank becomes distressed first. The upper limit of 100 time steps is set as the model is designed for short time scales that prevent banks from adjusting their financial positions. While this limit is somehow arbitrary, in our case about 90% of simulations stop before reaching it. Finally note that the dynamics of the EDB model admits only a stationary state where all banks have defaulted, yet we are not interested in this situation unless this state is reached very quickly.
[57] T. Squartini and D. Garlaschelli, New Journal of Physics **13**, 083001 (2011).
[58] G. Cimini, T. Squartini, D. Garlaschelli, and A. Gabrielli, Scientific Reports **5**, 15758 (2015).
[59] L. C. Freeman, Sociometry **40**, 35 (1977).
[60] We report only result for the first economic scenario LC-LD, since the other two scenarios produce similar results.
[61] G. A. Vento and P. La Ganga, "New issues in financial and credit markets," (Palgrave Macmillan UK, 2010) Chap. Inter-bank Market and Liquidity Distribution during the Great Financial Crisis: The e-MID Case, pp. 82–98.
[62] P. Barucca and F. Lillo, Chaos, Solitons & Fractals **88**, 244 (2016).